

## **Comparison of Imaging Parameters between OCT, GDx and HRT in the Northern Finland Birth Cohort Eye Study**

Katri Stoor MD, Department of Ophthalmology, PEDEGO research unit and Medical research center, University of Oulu and Oulu University Hospital

Elina Karvonen MD, Department of Ophthalmology, PEDEGO research unit and Medical research center, University of Oulu and Oulu University Hospital

Ilmari Leiviskä BSc, Department of Ophthalmology, PEDEGO research unit and Medical research center, University of Oulu and Oulu University Hospital

Johanna Liinamaa MD, PhD, Department of Ophthalmology, PEDEGO research unit and Medical research center, University of Oulu and Oulu University Hospital

Ville Saarela MD, PhD, Department of Ophthalmology, PEDEGO research unit and Medical research center, University of Oulu and Oulu University Hospital

Correspondence: Katri Stoor, MD

Department of Ophthalmology

Box 21, Oulu University Hospital

90029 Oulu

+358505449253

## Abstract

*Purpose:* The purpose of the study was to assess and compare the optic nerve head (ONH) and retinal nerve fiber layer (RNFL) parameters and image quality parameters obtained by Cirrus HD-OCT, GDxECC and HRT3 in a population-based screening study.

*Methods:* This analysis examined 2566 subjects taking part in the Northern Finland Birth Cohort Eye study. Images with spectral domain OCT (Cirrus HD-OCT 4000), scanning laser ophthalmoscopy (HRT3) and scanning laser polarimetry (GDxECC) were obtained from each subject. The correlation of average and regional parameters of RNFL and ONH between devices was evaluated.

*Results:* The RNFL thickness was 90.9  $\mu\text{m}$  when measured with OCT, 24.6  $\mu\text{m}$  with HRT and 48.1  $\mu\text{m}$  with GDx. There was high correlation between the disc and cup measurements with the HRT and OCT and the RNFL thickness of the OCT and GDx ( $r > 0.5$ ). A statistically significant correlation was found between RNFL measurements of the HRT and OCT in the superior, temporal and inferior quadrants. OCT signal strength correlated with the image quality parameters of the HRT and GDx. The percentage of good quality images was the lowest with the GDx.

*Conclusion:* The RNFL thickness in Northern Finland birth cohort was at a lower level compared to other studies. The study confirms the difference in measuring ONH parameters between the imaging devices. However, significant correlations between devices were found in the cup volume and cup disc area ratio parameters of the OCT and HRT. The correlations between image quality parameters and glaucoma detection parameters were relatively low.

**Keywords:** retinal nerve fibre layer, optic nerve head, OCT, GDx, HRT

## Introduction

Glaucoma is defined as a group of progressive neuropathies characterized by damage to the retinal nerve fiber layer (RNFL). The destruction of ganglion cells and their axons results in typical changes in optic nerve head (ONH) and visual fields (VF). It has been recognized for several decades that the structural changes in the RNFL and in the optic disc precede functional changes in the visual fields. (Coleman et al., 1996; Quigley et al., 1980; Sommer et al., 1991; Tuulonen et al., 1993; T. G. Zeyen & Caprioli, 1993).

The structural changes in the optic disc and nerve fibers have traditionally been detected and monitored using ONH and RNFL photography. These methods have certain disadvantages. They do not provide quantitative measurements and the detection of diffuse RNFL loss is challenging (Jonas & Dichtl, 1996). Moreover, the evaluation of photographs is subject to interobserver variability (Azua-Blanco et al., 2003; Coleman et al., 1996; T. Zeyen et al., 2003). Alternative imaging methods: optical coherence tomography (OCT), scanning laser polarimetry (GDx) and scanning laser ophthalmoscopy (HRT), may offer means to overcome these flaws. The imaging technology is different in each of these devices, but to some extent they produce analogous parameters. However, these parameters cannot be directly compared between devices. For example, the RNFL is estimated thicker by the OCT compared to HRT and GDx (Leung et al., 2010; Schallenberg et al., 2013).

There are studies comparing the results of the devices in glaucomatous populations (Fanihagh et al., 2015; Leung et al., 2010; Schallenberg et al., 2013). However, there is limited knowledge on the comparability of the imaging parameters in a normal population, especially utilizing the more recent generations of the OCT, HRT and GDx. Moreover, the devices use different methods to assess image quality, including the strength of the returning signal and inter-measurement

variability. The correlation between these quality evaluation methods has not been assessed in the literature.

The purpose of this study is to report both RNFL and ONH measurements in an unselected, randomized, middle-aged population and to compare the average and regional parameters obtained with the recent models of OCT, HRT and GDx. We also performed an evaluation and comparison of image quality parameters of the imaging devices.

## **Materials and Method**

### *Subjects*

The subjects of this study were the participants of the Northern Finland Birth Cohort 1966 (NFBC) Eye Study. The Eye Study is a part of a large population-based birth cohort that originally consisted of 12 058 individuals born in the two northernmost provinces in Finland in 1966. (Rantakallio & Hartikainen-Sorri, 1981) Data has been collected since the 24th gestational week and the original data has been supplemented with clinical examinations at different ages as well as with postal questionnaires. In 2011, 10321 cohort members were still living in Finland and 50% of them (5155) were randomized to the Eye Study, with 60% of the selected subjects (3070) participating to the eye examination between 2012 and 2015. In addition to imaging with fundus photography (stereoscopic ONH, RNFL, color and black-and-white photography), OCT, HRT and GDx, the eye study included an examination of best corrected visual acuity, intraocular pressure with a rebound tonometer and a Goldmann applanation tonometer, measurement of the corneal thickness and visual field examinations with standardized automated perimetry. The pupils were dilated for imaging. Ocular morbidity was evaluated from the fundus photographs by two ophthalmologists in a masked fashion. Glaucomatous findings were confirmed by glaucoma

specialists. The evaluation process has been described previously in detail (Saarela et al., 2013). Written, informed consent was obtained from all subjects following the tenets of the Declaration of Helsinki, and the study has been approved by the ethical committee of the Northern Ostrobothnia Hospital District.

### *OCT*

Cirrus HD-OCT 4000 (software V.6.0.0; Carl Zeiss Meditech AG, Oberkochen, Germany) is a spectral domain OCT that was used to obtain images of the optic disc and retina. OCT applies the principle of indirect interferometry to determine the interface between different ocular tissues. The device measures the RNFL thickness in a circle with a diameter of 3.46 mm centered at the optic disc. Optic Disc Cube 200 x 200 protocol was used. In addition to the RNFL average measurement, OCT imaging provides information on optic disc size and rim area. Images with a signal strength of 7-10 were included in the parameter analysis.

### *HRT*

Confocal scanning laser ophthalmoscopy was performed with HRT3 (Heidelberg Engineering, Heidelberg, Germany). The device projects a laser to record multiple layers of focal depths and it generates a 3-dimensional image of the surface of the optic nerve and the surrounding tissues, with the final topography image being the average of three measured topography images. A contour line was drawn on the inner edge of the scleral ring by an experienced ophthalmic photographer trained for this purpose. When the contour line is set, the software automatically calculates the optic disc and RNFL measurements.

The HRT uses topography standard deviation (TSD) to evaluate image quality. TSD is the mean standard deviation of each measurement point of the three topography images obtained by the device; the lower the standard deviation, the better the topography image. All images included in the study had an image quality  $\leq 40\mu\text{m}$ . For comparisons between the devices, the mean values of the inferonasal and inferotemporal RNFL thicknesses were calculated to form the inferior RNFL thickness. Similar calculation was performed for the superonasal and superotemporal segments to determine the superior RNFL thickness. HRT analyzes potential glaucomatous damage in the ONH by using Moorfields Regression Analysis (MRA) and Glaucoma Probability Score (GPS).

### *GDx*

Scanning laser polarimetry was carried out with the GDxPRO with Enhanced Corneal Compensation (ECC) (Carl Zeiss Meditec AG, Oberkochen, Germany). The measurement is based on the retardation of the polarized illuminating laser light along one axis by the birefringent retinal nerve fiber layer. The retardation of the backscattered light is proportional to the thickness of the RNFL. The required image quality for parameter analysis for the GDx was 8. The temporal-superior-nasal-inferior-temporal (TSNIT) plot displays RNFL thicknesses throughout the peripapillary measurement circle as an average RNFL thickness. Since GDx employs a different anatomical segmentation of the RNFL in comparison to the other devices, the GDx was not included in the segmentation analysis. The nerve fiber index (NFI) is the GDx parameter which has been developed to estimate glaucomatous damage.

### *Statistical analysis*

The study includes two entities. Firstly, the analysis of the correlation of imaging parameters between the devices. For this analysis the inclusion criteria was a good image quality and one

randomized eye was accepted for each subject. Secondly, we evaluated the correlation of image quality parameters. For this study all imaged eyes were included (Fig.1). Ocular morbidity was not an exclusion criteria in the study.

Statistical analysis was performed with SPSS for Windows (Version 27, Armonk, NY). The linear relationship between parameters was assessed with Pearson correlation. Spearman rank correlation was used for analyzing non-linear relationships, for example the correlation of NFI of the GDx with HRT glaucoma analysis parameters (MRA and GPS). The agreements between the parameters of different devices were analyzed also visually with the Bland-Altman plots, where the Limits of Agreement (LOA) were defined as:  $\text{mean} \pm 1.96 * \text{standard deviation}$ . The mean change and 95% confidence intervals for HRT TSD and the OCT and GDx image quality parameters were calculated. Linear regression models were used to compute numerical results between the image quality parameters. A p-value  $< 0.05$  was considered statistically significant. The RNFL thickness was the only identical parameter between the three devices. The statistical difference of means between the three devices was analysed with ANOVA.

## **Results**

Good quality images from all three devices were achieved from 2566 subjects. One eye of each subject was randomized for this analysis. 1398 subjects (54.5%) were females. The sample size for the image quality analysis was 5231 eyes (Fig.1).

### *Global parameters*

The average RNFL thicknesses measured with HRT, OCT and GDx were 24.6  $\mu\text{m}$ , 90.9  $\mu\text{m}$  and 48.1  $\mu\text{m}$ , respectively (Table 1, Fig. 2). The difference in means (ANOVA) was statistically significant ( $p < 0.001$ ). There was a strong correlation in the cup disc ratio parameters measured with HRT and OCT (HRT cup disc area ratio vs. OCT average cup disc ratio  $r 0.827$ ,  $p < 0.001$ , HRT linear cup disc ratio vs. OCT average cup disc ratio  $r 0.852$   $p < 0.001$  and HRT vertical cup disc ratio vs. OCT vertical cup disc ratio  $r 0.800$ ,  $p < 0.001$ ) as well as in the cup volume parameter ( $r 0.91$ ,  $p < 0.001$ ). The correlation of disc area measurements of HRT and OCT was statistically significant,  $r 0.655$ ,  $p < 0.001$  and the correlation between HRT rim volume and OCT average RNFL thickness was also statistically significant, yet weak,  $r 0.118$ ,  $p < 0.001$ .

The TSNIT average of the GDx had statistically significant, although weak, correlations with HRT mean RNFL thickness and cross-sectional area,  $r 0.138$  and  $0.128$ , respectively,  $p < 0.001$ . The correlation between OCT average RNFL thickness and GDx TSNIT average was  $r 0.527$ ,  $p < 0.001$ . The results are summarized in Table 2 and Figure 3. The correlation of TSNIT average with the RNFL thickness parameters of OCT and HRT was improved with increasing image quality.

#### *Sectoral and glaucoma probability parameters*

Sectoral parameters (superior, temporal, inferior and nasal) were compared between HRT and OCT. The correlation was highest in temporal sector  $r 0.344$  ( $p < 0.001$ ). The correlations between superior and inferior sector were statistically significant, but weak:  $r 0.134$  ( $p < 0.001$ ) and  $r 0.189$  ( $p < 0.001$ ). The correlation of nasal sector was not statistically significant,  $r -0.033$  ( $p = 0.091$ ). The correlation between glaucoma probability parameters NFI and MRA was  $r -0.143$  ( $p < 0.001$ ) and NFI and GPS  $r 0.176$  ( $p < 0.001$ ).



### *Image quality parameters*

There were 12 (0.23%) poor-quality images obtained with OCT, 71 (1.3%) with HRT and 241 (4.6%) with GDx. Pearson correlation for the image quality parameters was not statistically significant between HRT and GDx,  $r = -0.017$  ( $p = 0.224$ ). The signal strength of the OCT showed a statistically significant correlation with GDx overall score ( $r = 0.075$ ,  $p < 0.001$ ) and HRT TSD ( $r = -0.180$ ,  $p < 0.001$ ). Per one unit increase in the OCT signal strength, the estimated change in HRT TSD was  $-3.2$  (CI 95%  $-3.6$  to  $-2.8$ ) and the change in GDx overall score was  $0.22$  (CI 95%  $0.15$  -  $0.3$ ). Per one unit increase in the GDx overall score, the change in HRT TSD was  $-0.17$  (CI 95%  $-0.32$  to  $-0.04$ ). The agreement of good quality images was 98.5% between HRT and OCT, 95.3% between GDx and OCT and 94.3% between HRT and GDx the agreement. The results of the image quality analysis are summarized in Fig. 4 and Table 3.

### **Discussion**

In this study, we report the average RNFL thickness measured with Cirrus HD-OCT 4000, HRT3 and GDxECC in a large, middle-aged population. As has been previously reported, the OCT showed the highest whereas the HRT exhibited the lowest values for mean RNFL thickness (Fanihagh et al., 2015).

An Australian study found the average RNFL to be  $99.4 \mu\text{m}$  using the same model Cirrus HD-OCT 4000 when examining young adults (Tariq et al., 2012). The other studies using different Spectral Domain OCTs report different thicknesses varying from  $90.1 \mu\text{m}$  to  $102.4 \mu\text{m}$  (Bendschneider et al., 2010; Knight et al., 2012; Li et al., 2020; Ocansey et al., 2020). The RNFL thickness in the present study ( $90.9 \mu\text{m}$ ) is small compared to previous reports. Knight et al. described a low RNFL thickness ( $90.1 \mu\text{m}$ ) in their study when assessing a subgroup of normal

subjects of European descent with mean age of 49.1 (Knight et al., 2012). Considering that the mean yearly decrease in RNFL thickness is 0.365  $\mu\text{m}$  (95% CI 0.26-0.47) (Celebi & Mirza 2013) the result is almost identical with ours.

The TSNIT average of healthy people has been assessed with GDxECC in previous studies. Rao et al. examined 140 eyes of 73 Indian subjects and Bertuzzi studied 70 subjects in Italy (Bertuzzi et al., 2014; Rao et al., 2014). The TSNIT averages were 49.4  $\mu\text{m}$  and 50.2  $\mu\text{m}$ , respectively, which are somewhat higher than our result of 48.1  $\mu\text{m}$ .

The RNFL thickness measured with HRT3 in our study was 24.6  $\mu\text{m}$ , which is similar to two recent publications. Columbo et al. examined hypertensive patients and Schulze et al. examined 60 healthy individuals. Both groups found a mean thickness of 24  $\mu\text{m}$  (Colombo et al., 2016; Schulze et al., 2015).

The differences in RNFL thickness measurements between devices are not unexpected because of the different measuring techniques and parameter definitions used by each device. OCT performs interferometry to discriminate between tissues with different optical properties in the retina. GDx is based on the principle of the polarized light passing through the birefringent RNFL undergoing a measurable phase retardation. Both these techniques evaluate RNFL from a signal produced within the retinal tissue. In contrast, the measurement technique of the HRT is completely different; it measures the topography of the surface of the retina. The edge of the ONH is defined by a contour line drawn manually on the topography image by the operator. The device calculates the position of a reference plane 50  $\mu\text{m}$  below the temporal edge of the ONH in order to distinguish between cup and rim. The RNFL thickness is defined as the mean RNFL thickness along the contour line, relative to the reference plane. The RNFL and most ONH parameters of the HRT are dependent on the position of the contour line and the reference

plane. Hence, with a very high position of the reference plane, the RNFL may occasionally reach negative values (Fig. 2).

Schallenberg et al. examined the correlation of GDxECC mean TSNIT versus Spectralis OCT RNFL average (Schallenberg et al., 2013). The Pearson correlation coefficient was 0.578. Similarly, in our study the correlation between GDxECC and Cirrus HD-OCT was 0.527. Fanihagh et al. compared RNFL parameters in 114 glaucoma patients. They reported a correlation between Cirrus OCT and GDxECC of 0.589, which is also in concordance with our result. The correlations between Cirrus OCT and HRT3 (0.397) and GDxECC and HRT3 (0.293) were higher than in our study with correlations of 0.162 and 0.128, respectively.

Due to the different segmentation of the GDx, we compared the regional parameters only between OCT and HRT. The best correlation was found in temporal RNFL, 0.344. This is in concurrence with Fanihagh et al., who reported correlations below 0.4 in the superior and inferior regional parameters between OCT and HRT.

HRT and OCT showed good correlations regarding the parameters of cup disc ratio and cup volume (0.862 and 0.910, respectively). The correlation of rim area was poorer (0.337). The HRT evaluates the neural rim from the topography not from measurements within the retina as is the case with OCT. This may explain the lower correlation observed in rim area measurements. Few articles have compared the ONH parameters between Cirrus and HRT3 and also in previous papers the lower correlation of rim area has been described. Sato et al. performed a study comparing ONH parameters (disc area, rim area, cup to disc ratio and cup volume) using HRT3 and Cirrus HD-OCT. They found highly significant Pearson correlations in the range of  $r = 0.668$  to  $0.820$  compared to ours  $0.337$  to  $0.910$ , but the Bland-Altman analysis revealed a poor agreement with the exception of the cup to disc ratio (Sato et al., 2012). In addition, Kraatz et

al. found that the correlations of the same parameters were in the range of 0.65 to 0.88. (Kratz et al., 2014)

Calvo et al. reported ONH parameters measured with HRT3 and Cirrus OCT in 182 normal subjects. In their study, Cirrus OCT and HRT3 measured very similar values for rim area and disc area. Rim area was 1.49 mm<sup>3</sup> with OCT and 1.50 mm<sup>3</sup> with HRT3, disc area was 1.93 mm<sup>3</sup> with OCT and 1.87 mm<sup>3</sup> with HRT3. In our study, HRT3 estimated higher rim and disc areas compared to OCT. The mean cup disc ratio in Calvo's study was 0.42 with OCT and 0.19 with HRT3 which is in concordance with our values of 0.50 with OCT and 0.20 with HRT3 (Calvo et al., 2014).

The HRT and GDx provide summary parameters specifically developed to measure glaucomatous damage. As far as we are aware, this is the first study reporting these correlations in a normal population. The glaucoma probability parameter of GDx, the Nerve Fiber Indicator (NFI), is a global measure based on the entire RNFL thickness map. HRT offers two glaucoma probability parameters, Moorfields Regression Analysis (MRA) and Glaucoma Probability Score (GPS). MRA analyses the regression of the logarithm of the global and six sectoral rim areas to the matching disc areas and compares the results to a normative database defining the area as normal, borderline and outside normal limits. GPS provides an automated interpretation of ONH topography combining the horizontal and vertical curvature of the RNFL with the steepness, size and depth of the cup (Swindale et al., 2000). Despite the different parameter definitions, we found a statistically significant, although weak correlation between NFI and the two HRT parameters. The MRA is a statistical analysis of the rim area with respect to disc area, the GPS evaluates the shape of the overall topography of the optic cup and NFI is a statistical analysis of the RNFL. All parameters have been shown to correlate with glaucomatous damage. However, due to the different definitions their mutual correlation is low. OCT does not offer a numerical glaucoma probability summary parameter. However, glaucomatous damages may be evaluated from OCT images from color-coded probabilities at the RNFL sectors. The predictive value of this

analysis has been shown to be low in the NFBC Eye Study (Karvonen et al. 2020). The diagnostic accuracy for glaucoma is similar for OCT, GDx and HRT (Michelessi et al. 2015). However, there is a progressive lack of interest in both HRT and GDx.

There was substantial variation in the capabilities of the devices to produce sufficient quality images. According to our results, it is more difficult to achieve good quality imaging with GDx than with the other two devices. Despite the fact that the population consisted of randomized middle-aged subjects, 4.6% had poor image quality with the GDx. This is noticeably higher compared to HRT (1.4%) and OCT (0.2%). There was a statistically significant correlation between image quality measurements between the devices except those between the HRT and GDx. Even with these two devices, there was a correlation in image quality with GDx overall score values above 3. However, the subjects with very low GDx image quality (overall score 1) had fairly good HRT TSD values (Fig. 4) which affected the total correlation. This would indicate that in these subjects the GDx polarimetry measurements from within the RNFL failed, but the topography measurements of the HRT from the surface of the RNFL were successful.

The fundamental strength of the present study is the birth cohort. The sample size is large and the population randomized and of the same age and ethnicity. Current imaging technology was used to perform the examinations for all the subjects. Only 60% of the randomized subjects took part in the study, which may be considered a limitation. However, a participation rate of over 50% is considered good especially in a birth cohort with progressive follow-up and repeated examinations.

In conclusion, the mean RNFL thickness in the Northern Finland birth cohort was at a lower level in comparison to other published studies. The study confirms that there are differences in measuring ONH parameters when utilizing different imaging devices. The differences are explained by different measurement techniques and parameter definitions, and they are also

present in cases with excellent image quality. The parameters displaying the highest correlations were the cup volume and cup disc area ratio parameters as assessed by OCT and HRT. Despite being statistically significant, the correlations between image quality parameters and glaucoma detection parameters were relatively low.

### **Acknowledgements**

This study was supported by Glaukoma Tukisäätiö Lux, Silmäsäätiö Foundation and the Competitive State Research Financing of the Expert Responsibility area of Oulu University Hospital.

### **References**

Azuara-Blanco A, Katz LJ, Spaeth GL, Vernon SA, Spencer F & Lanzl IM (2003): Clinical agreement among glaucoma experts in the detection of glaucomatous changes of the optic disk using simultaneous stereoscopic photographs. *American Journal of Ophthalmology* **136**: 949-950.

Bendschneider D, Tornow RP, Horn FK, Laemmer R, Roessler CW, Juenemann AG, Kruse FE & Mardin CY (2010): Retinal nerve fiber layer thickness in normals measured by spectral domain oct. *Journal of Glaucoma* **19**: 475-482.

Bertuzzi F, Benatti E, Esempio G, Rulli E & Miglior S (2014): Evaluation of retinal nerve fiber layer thickness measurements for glaucoma detection: GDx ECC versus spectral-domain OCT. *Journal of Glaucoma* **23**: 232-239.

Calvo P, Ferreras A, Abadia B, Ara M, Figus M, Pablo LE & Frezzotti P (2014): Assessment of the optic disc morphology using spectral-domain optical coherence tomography and scanning laser ophthalmoscopy. *BioMed Research International* **2014**.

Celebi ARC & Mirza GE (2013): Age-related change in retinal nerve fiber layer thickness measured with spectral domain optical coherence tomography. *Investigative Ophthalmology and Visual Science* **54**: 8095-8103.

Coleman AL, Sommer A, Enger C, Knopf HL, Stamper RL & Minckler DS (1996): Interobserver and intraobserver variability in the detection of glaucomatous progression of the optic disc. *Journal of Glaucoma* **5**: 384-389.

Colombo L, Bertuzzi F, Rulli E & Miglior S (2016): Correlations between the individual risk for glaucoma and RNFL and optic disc morphometrical evaluations in ocular hypertensive patients. *Journal of Glaucoma* **25**: e455-e462.

Fanihagh F, Kremmer S, Anastassiou G, Schallenberg M, Steuhl K-P & Selbach M (2015): Optical coherence tomography, scanning laser polarimetry and confocal scanning laser ophthalmoscopy in retinal nerve fiber layer measurements of glaucoma patients. *Open Ophthalmology Journal* **9**: 41-48.

Jonas JB & Dichtl A (1996): Evaluation of the retinal nerve fiber layer. *Survey of Ophthalmology* **40**: 369-378.

Karvonen E, Stoor K, Luodonpaa M, Hagg P, Lintonen T, Liinamaa J, Tuulonen A & Saarela V (2020): Diagnostic performance of modern imaging instruments in glaucoma screening. *British Journal of Ophthalmology* **104**: 1399-1405.

Knight OJ, Girkin CA, Budenz DL, Durbin MK & Feuer WJ (2012): Effect of race, age, and axial length on optic nerve head parameters and retinal nerve fiber layer thickness measured by cirrus HD-OCT. *Archives of Ophthalmology* **130**: 312-318.

Kratz A, Lim R & Goldberg I (2014): Optic nerve head assessment: Comparison of Cirrus optic coherence tomography and Heidelberg Retinal Tomograph 3. *Clinical and Experimental Ophthalmology* **42**: 734-744.

Leung CK -s., Ye C, Weinreb RN, Cheung CYL, Qiu Q, Liu S, Xu G & Lam DSC (2010): Retinal Nerve Fiber Layer Imaging with Spectral-Domain Optical Coherence Tomography. A Study on Diagnostic Agreement with Heidelberg Retinal Tomograph. *Ophthalmology* **117**: 267-274.

Li D, Rauscher FG, Choi EY, et al. (2020): Sex-Specific Differences in Circumpapillary Retinal Nerve Fiber Layer Thickness. *Ophthalmology* **127**: 357-368.

Michelessi M, Lucenteforte E, Oddone F, Brazzelli M, Parravano M, Franchi S, Ng SM & Virgili G (2015): Optic nerve head and fibre layer imaging for diagnosing glaucoma. *Cochrane Database of Systematic Reviews* **2015**.

Ocansey S, Abu EK, Owusu-Ansah A, et al. (2020): Normative Values of Retinal Nerve Fibre Layer Thickness and Optic Nerve Head Parameters and Their Association with Visual Function in an African Population. *Journal of Ophthalmology* **2020**.



Quigley HA, Miller NR & George T (1980): Clinical Evaluation of Nerve Fiber Layer Atrophy as an Indicator of Glaucomatous Optic Nerve Damage. *Archives of Ophthalmology* **98**: 1564-1571.

Rantakallio P & Hartikainen-Sorri A-L (1981): The relationship between birth weight, smoking during pregnancy and maternal weight gain. *American Journal of Epidemiology* **113**: 590-595.

Rao HL, Venkatesh CR, Vidyasagar K, Yadav RK, Addepalli UK, Jude A, Senthil S & Garudadri CS (2014): Retinal nerve fiber layer measurements by scanning laser polarimetry with enhanced corneal compensation in healthy subjects. *Journal of Glaucoma* **23**: 589-593.

Saarela V, Karvonen E, Stoor K, Hägg P, Luodonpää M, Kuoppala J, Taanila A & Tuulonen A (2013): The Northern Finland Birth Cohort Eye Study: Design and baseline characteristics. *BMC Ophthalmology* **13**.

Sato S, Hirooka K, Baba T & Shiraga F (2012): Comparison of optic nerve head parameters using Heidelberg Retina Tomograph 3 and spectral-domain optical coherence tomography. *Clinical and Experimental Ophthalmology* **40**: 721-726.

Schallenberg M, Dekowski D, Kremmer S, Selbach JM & Steuhl KP (2013): Comparison of Spectralis-OCT, GDxVCC and GDxECC in assessing retinal nerve fiber layer (RNFL) in glaucomatous patients. *Graefe's Archive for Clinical and Experimental Ophthalmology* **251**: 1343-1353.

Schulze A, Lamparter J, Pfeiffer N, Berisha F, Schmidtman I & Hoffmann EM (2015): Comparison of Laser Scanning Diagnostic Devices for Early Glaucoma Detection. *Journal of Glaucoma* **24**: 442-447.

Sommer A, Katz J, Quigley HA, Miller NR, Robin AL, Richter RC & Witt KA (1991): Clinically Detectable Nerve Fiber Atrophy Precedes the Onset of Glaucomatous Field Loss. *Archives of Ophthalmology* **109**: 77-83.

Swindale NV, Stjepanovic G, Chin A & Mikelberg FS (2000): Automated analysis of normal and glaucomatous optic nerve head topography images. *Investigative Ophthalmology and Visual Science* **41**: 1730-1742.

Tariq YM, Li H, Burlutsky G & Mitchell P (2012): Retinal nerve fiber layer and optic disc measurements by spectral domain OCT: Normative values and associations in young adults. *Eye (Basingstoke)* **26**: 1563-1570.

Tuulonen A, Lehtola J & Airaksinen PJ (1993): Nerve Fiber Layer Defects with Normal Visual Fields: Do Normal Optic Disc and Normal Visual Field Indicate Absence of Glaucomatous Abnormality? *Ophthalmology* **100**: 587-598.

Zeyen TG & Caprioli J (1993): Progression of Disc and Field Damage in Early Glaucoma. *Archives of Ophthalmology* **111**: 62-65.

Zeyen T, Miglior S, Pfeiffer N, Cunha-Vaz J & Adamsons I (2003): Reproducibility of evaluation of optic disc change for glaucoma with stereo optic disc photographs. *Ophthalmology* **110**: 340-344.

Figure legends:

Fig. 1. Flow chart of the study population

Fig 2. Comparison of RNFL thickness measurements

Fig.3. Bland-Altman plots of disc area, rim area, cup volume and RNFL parameters. LOA = Limit of agreement.

Fig 4. Graphical presentation of the measurements of image quality (N = 5231). The gray lines (A, C, E) represent the correlations between image quality parameters. The vertical and horizontal lines (B, D, F) indicate the cut-off values of the image quality for each device. GDx Overall Scores of 2 or 3 were not detected. A slight jittering was used for visualization.

Table 1. Baseline characteristics of the study population (N=2566).

	Mean (N)	SD (%)
Age	47.5	0.9
CCT	535	35
IOP	14.9	3.5
Spherical equivalent	-1.3	2.4
Glaucoma	(23)	(0.9 %)
Diabetes <sup>1</sup>	(116)	(4.5 %)

<sup>1</sup>Missing diabetes data from 283 individuals.

Table 2. Descriptive statistics for the parameters (N=2566 eyes).

	Mean or Median	SD or range
<b>Global parameters</b>		
HRT disc area (mm <sup>2</sup> )	2.2	0.5
HRT rim area (mm <sup>2</sup> )	1.7	0.3
HRT cup disc area ratio*	0.20	0.01 to 0.93
HRT linear cup disc ratio*	0.44	0.01 to 0.96
HRT cup volume (mm <sup>3</sup> )*	0.07	0.01 to 1.03
HRT rim volume (mm <sup>3</sup> )	0.46	0.16
HRT vertical cup disc ratio*	0.35	0.01 to 0.93
HRT mean RNFL thickness (μm)	24.6	6.4
HRT RNFL cross-sectional area (mm <sup>2</sup> )	1.3	0.34
OCT disc area (mm <sup>2</sup> )	1.8	0.3
OCT rim area (mm <sup>2</sup> )	1.3	0.2
OCT average cup disc ratio*	0.50	0.06 to 0.85
OCT cup volume (mm <sup>3</sup> )*	0.10	0.01 to 1.17
OCT vertical cup disc ratio *	0.47	0.04 to 0.87
OCT average RNFL thickness (μm)	90.9	9.5
GDx TSNIT average (μm)	48.1	4.7
<b>Sectorial parameters</b>		
HRT temporal mean RNFL thickness (μm)	8.3	2.5
HRT superior mean RNFL thickness (μm)	30.6	8.1
HRT nasal mean RNFL thickness (μm)	28.6	9.4
HRT inferior mean RNFL thickness (μm)	31.0	8.6
OCT temporal RNFL quadrant (μm)	64.7	11.8
OCT superior RNFL quadrant (μm)	113.2	15.9
OCT nasal RNFL quadrant (μm)	68.8	11.9
OCT inferior RNFL quadrant (μm)	116.9	16.6
<b>Glaucoma probability parameters</b>		
HRT Moorfields regression analysis (MRA)	0.1	0.029
HRT Glaucoma probability score (GPS)*	0.12	0.09 to 0.36
GDx Nerve Fiber Indicator (NFI)*	22	16 to 28
<b>Quality parameters (From all eligible eyes, N=5321)</b>		
HRT topography standard deviation (TSD)	12	6 to 117
OCT signal strength	10	6 to 10
GDx overall score	9	1 to 10

Data presented as mean and standard deviation, SD. \*In the case of non-normal data, median and range from minimum to maximum values were used.

Table 3. Pearson's correlation coefficients between parameters

<b>Global parameters</b>		r	P
HRT disc area	OCT disc area	0.655	<0.001
HRT rim area	OCT rim area	0.337	<0.001
HRT cup disc area ratio	OCT average cup disc ratio	0.862*	<0.001
HRT linear cup disc ratio	OCT average cup disc ratio	0.852	<0.001
HRT cup volume	OCT cup volume	0.910	<0.001
HRT rim volume	OCT average RNFL thickness	0.118	<0.001
HRT vertical cup disc ratio	OCT vertical cup disc ratio	0.800	<0.001
HRT mean RNFL thickness	OCT average RNFL thickness	0.162	<0.001
HRT mean RNFL thickness	GDx TSNIT average	0.138	<0.001
HRT RNFL cross-sectional area	OCT average RNFL thickness	0.197	<0.001
HRT RNFL cross-sectional area	GDx TSNIT average	0.128	<0.001
OCT RNFL thickness	GDx TSNIT average	0.527	<0.001
<b>Sectorial parameters</b>			
HRT temporal mean RNFL thickness	OCT temporal RNFL quadrant	0.344	<0.001
HRT superior mean RNFL thickness	OCT superior RNFL quadrant	0.134	<0.001
HRT nasal mean RNFL thickness	OCT nasal RNFL quadrant	-0.033	0.091
HRT inferior mean RNFL thickness	OCT inferior RNFL quadrant	0.189	<0.001
<b>Glaucoma probability parameters</b>			
HRT Moorfields regression analysis (MRA)	GDx Nerve Fiber Indicator (NFI)	-0.143*	<0.001
HRT Glaucoma probability score (GPS)	GDx Nerve Fiber Indicator (NFI)	0.176*	<0.001
<b>Image quality parameters</b>			
HRT topography standard deviation (TSD)	OCT signal strength	-0.180*	<0.001
HRT topography standard deviation (TSD)	GDx overall score	-0.017*	0.224
OCT signal strength	GDx overall score	0.075*	<0.001

P value for two sided test of significance.

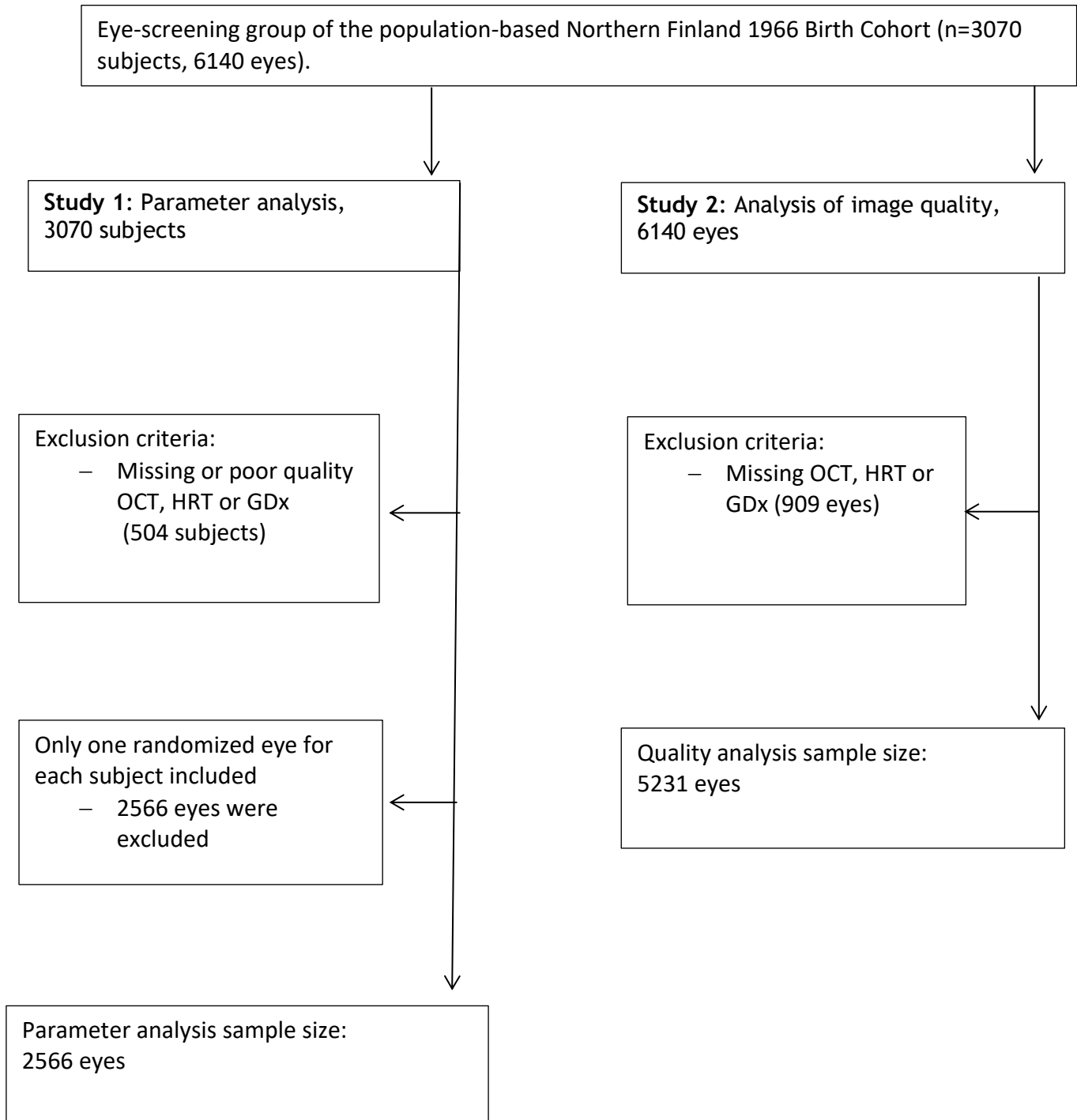
\* Spearman rank correlation for non-linear relationship.

Table 4. Classifications of image quality

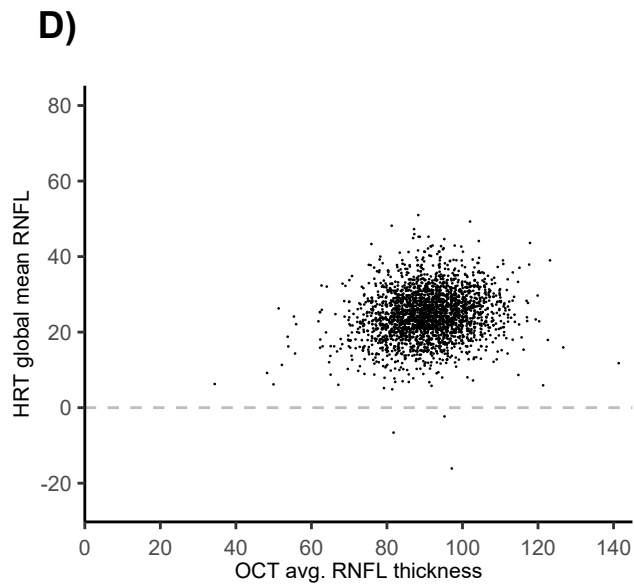
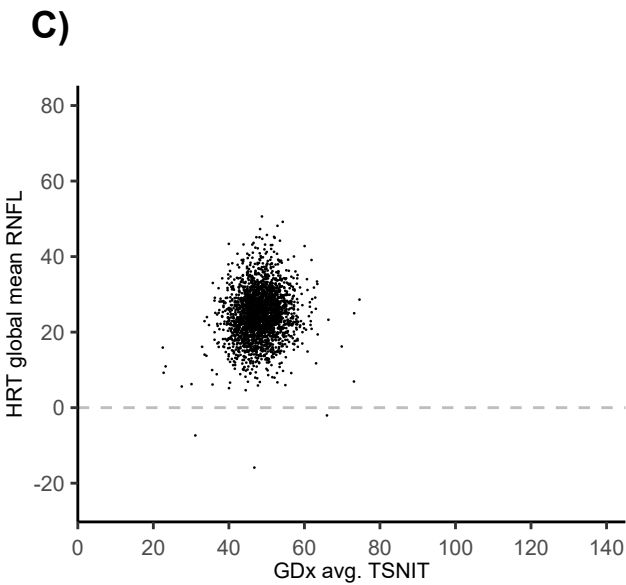
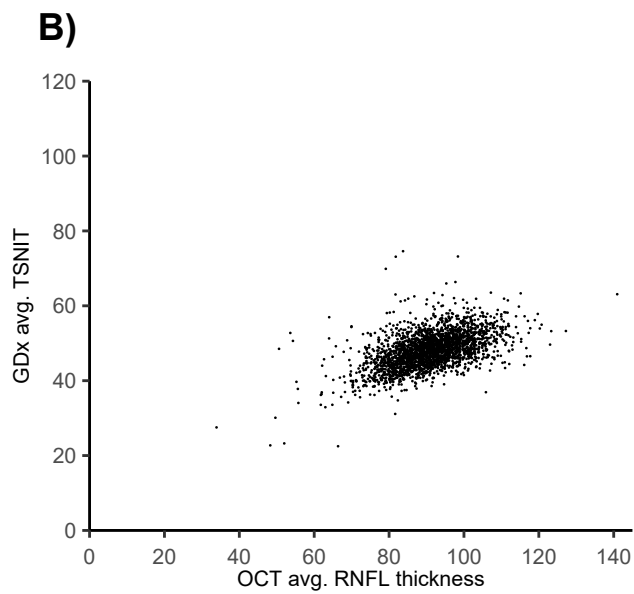
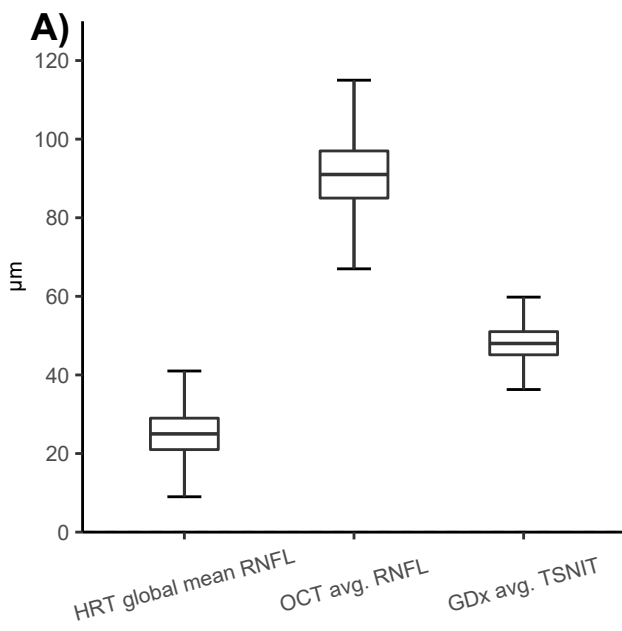
Paired comparisons for image quality classification					Disagreement* between devices, N (%)
OCT					
		Poor	Good	Total	
HRT	Poor	2	69	71	79/5231 (1.5 %)
	Good	10	5150	5160	
Total		12	5219	5231	
OCT					
		Poor	Good	Total	
GDx	Poor	4	237	241	245/5231 (4.7 %)
	Good	8	4982	4990	
Total		12	5219	5231	
GDx					
		Poor	Good	Total	
HRT	Poor	6	65	71	300/5231 (5.7 %)
	Good	235	4925	5160	
Total		241	4990	5231	

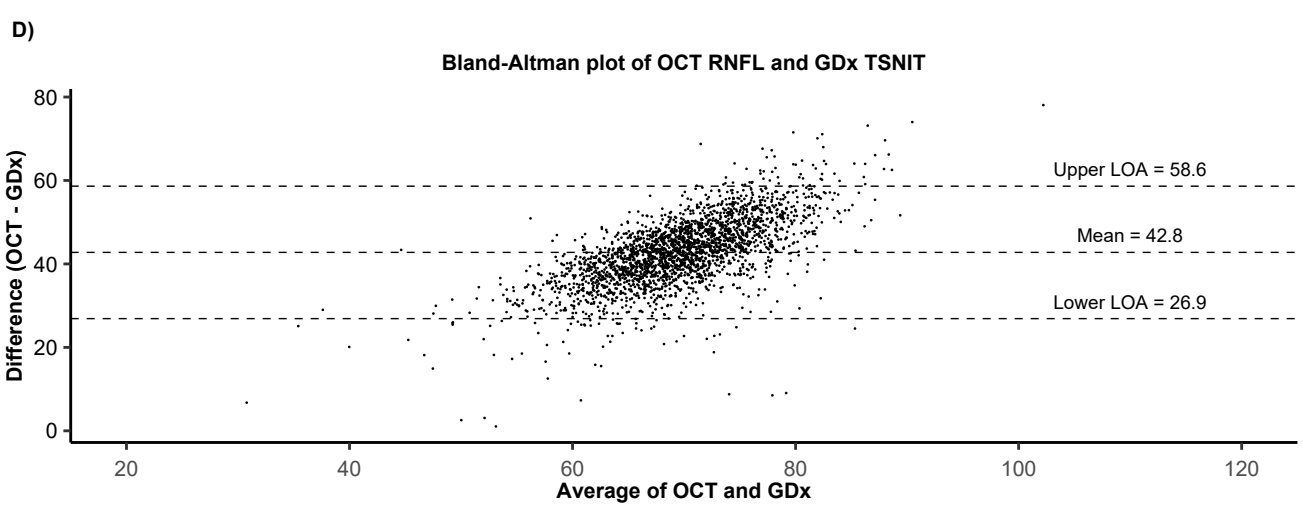
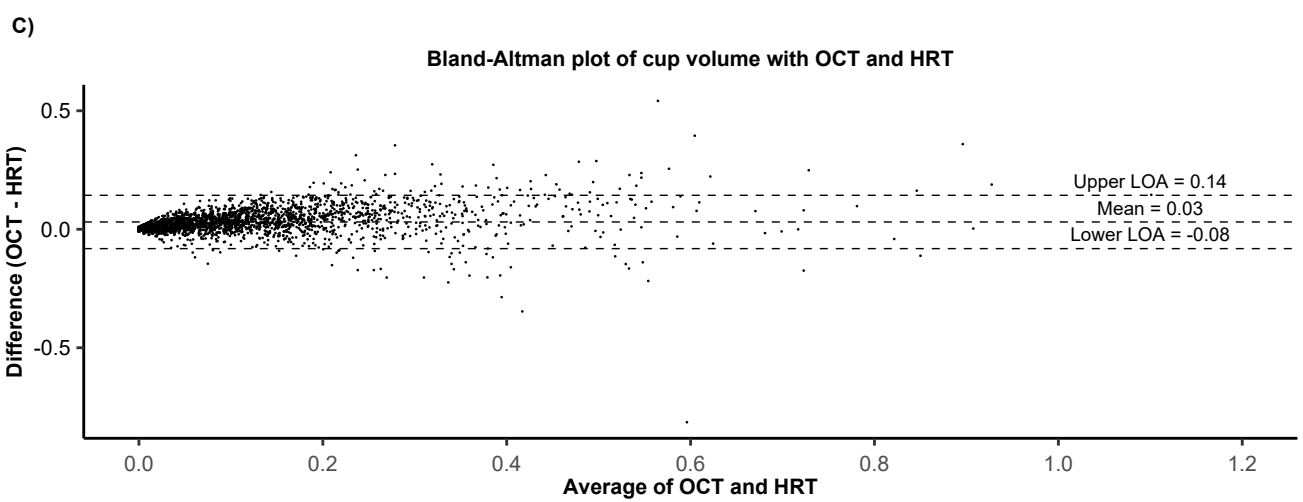
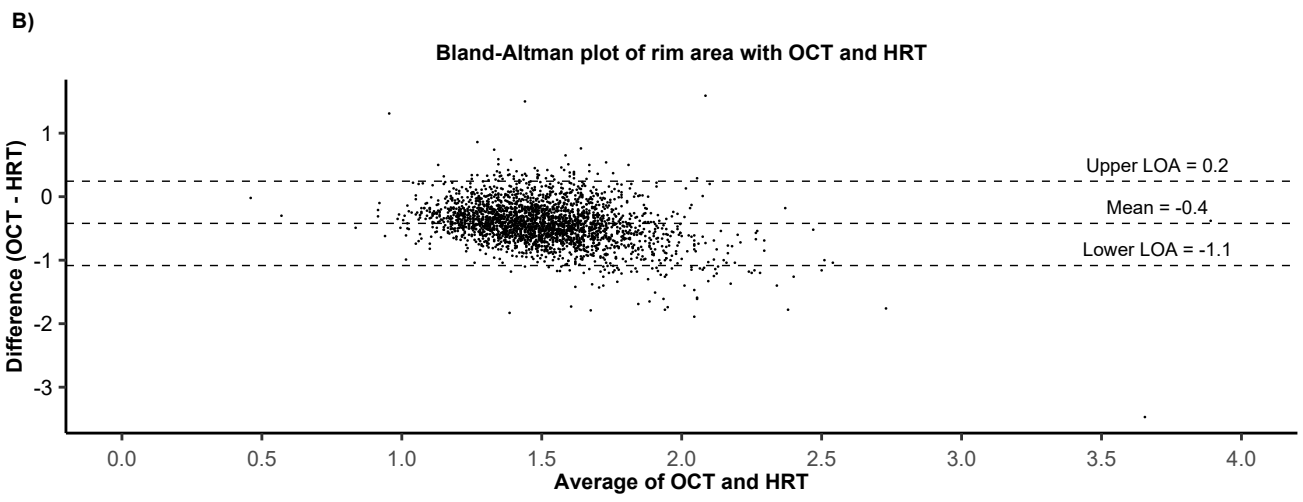
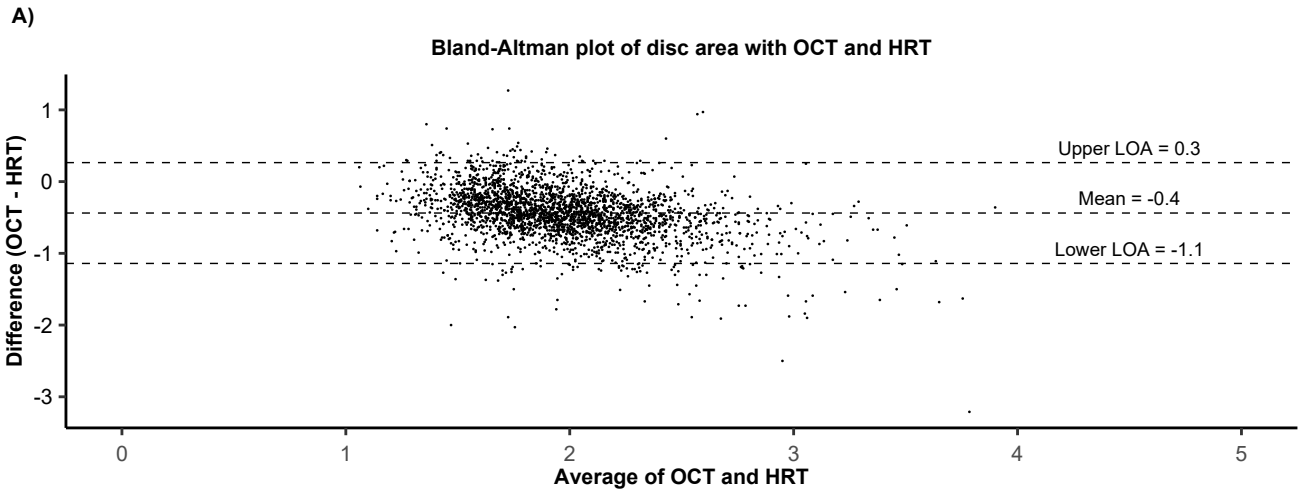
\*Disagreement calculated by dividing the sum of cross-classified values with the total classifications.

Figure 1.









A slight jittering was used for visualization.

